



Heriot-Watt University  
Research Gateway

# Photocatalytic reduction of CO<sub>2</sub> with H<sub>2</sub>O over graphene oxide-supported oxygen-rich TiO<sub>2</sub> hybrid photocatalyst under visible light irradiation

## Citation for published version:

Tan, LL, Ong, W-J, Chai, S-P & Mohamed, AR 2017, 'Photocatalytic reduction of CO<sub>2</sub> with H<sub>2</sub>O over graphene oxide-supported oxygen-rich TiO<sub>2</sub> hybrid photocatalyst under visible light irradiation: Process and kinetic studies', *Chemical Engineering Journal*, vol. 308, pp. 248-255.  
<https://doi.org/10.1016/j.cej.2016.09.050>

## Digital Object Identifier (DOI):

[10.1016/j.cej.2016.09.050](https://doi.org/10.1016/j.cej.2016.09.050)

## Link:

[Link to publication record in Heriot-Watt Research Portal](#)

## Document Version:

Peer reviewed version

## Published In:

Chemical Engineering Journal

## General rights

Copyright for the publications made accessible via Heriot-Watt Research Portal is retained by the author(s) and / or other copyright owners and it is a condition of accessing these publications that users recognise and abide by the legal requirements associated with these rights.

## Take down policy

Heriot-Watt University has made every reasonable effort to ensure that the content in Heriot-Watt Research Portal complies with UK legislation. If you believe that the public display of this file breaches copyright please contact [open.access@hw.ac.uk](mailto:open.access@hw.ac.uk) providing details, and we will remove access to the work immediately and investigate your claim.

## Accepted Manuscript

Photocatalytic Reduction of CO<sub>2</sub> with H<sub>2</sub>O Over Graphene Oxide–Supported Oxygen–Rich TiO<sub>2</sub> Hybrid Photocatalyst Under Visible Light Irradiation: Process and Kinetic Studies

Lling-Lling Tan, Wee-Jun Ong, Siang-Piao Chai, Abdul Rahman Mohamed

PII: S1385-8947(16)31286-4  
DOI: <http://dx.doi.org/10.1016/j.cej.2016.09.050>  
Reference: CEJ 15760

To appear in: *Chemical Engineering Journal*

Received Date: 23 June 2016  
Revised Date: 1 September 2016  
Accepted Date: 10 September 2016

Please cite this article as: L-L. Tan, W-J. Ong, S-P. Chai, A. Rahman Mohamed, Photocatalytic Reduction of CO<sub>2</sub> with H<sub>2</sub>O Over Graphene Oxide–Supported Oxygen–Rich TiO<sub>2</sub> Hybrid Photocatalyst Under Visible Light Irradiation: Process and Kinetic Studies, *Chemical Engineering Journal* (2016), doi: <http://dx.doi.org/10.1016/j.cej.2016.09.050>

This is a PDF file of an unedited manuscript that has been accepted for publication. As a service to our customers we are providing this early version of the manuscript. The manuscript will undergo copyediting, typesetting, and review of the resulting proof before it is published in its final form. Please note that during the production process errors may be discovered which could affect the content, and all legal disclaimers that apply to the journal pertain.



**Photocatalytic Reduction of CO<sub>2</sub> with H<sub>2</sub>O Over Graphene Oxide–Supported Oxygen–Rich TiO<sub>2</sub> Hybrid Photocatalyst Under Visible Light Irradiation: Process and Kinetic Studies**

*Lling-Lling Tan<sup>a</sup>, Wee-Jun Ong<sup>b</sup>, Siang-Piao Chai<sup>c\*</sup> and Abdul Rahman Mohamed<sup>d</sup>*

<sup>a</sup>Chemical Engineering, School of Engineering and Physical Sciences, Heriot-Watt University, Jalan Venna P5/2, Precinct 5, 62200 Putrajaya, Wilayah Persekutuan Putrajaya, Malaysia.

<sup>b</sup>Institute of Materials Research and Engineering (IMRE), Agency for Science, Technology and Research (A\*STAR), 2 Fusionopolis Way, Innovis, 138634, Singapore.

<sup>c</sup>Multidisciplinary Platform of Advanced Engineering, Chemical Engineering Discipline, School of Engineering, Monash University, Jalan Lagoon Selatan, 46500 Bandar Sunway, Selangor, Malaysia.

<sup>d</sup>Low Carbon Economy (LCE) Group, School of Chemical Engineering, Universiti Sains Malaysia, Engineering Campus, Seri Ampangan, 143000 Nibong Tebal, Pulau Pinang, Malaysia.

\*Corresponding author:

Tel: +603-55146234; Fax: +603-55146207

E-mail address: [chai.siang.piao@monash.edu](mailto:chai.siang.piao@monash.edu)

**Abstract**

The photoreduction of carbon dioxide ( $\text{CO}_2$ ) into hydrocarbon fuels was studied in a homemade photocatalytic system over 5 wt. % graphene oxide-doped oxygen-rich  $\text{TiO}_2$  (5GO-OTiO<sub>2</sub>) photocatalyst. The  $\text{CO}_2$  transformation process is a sequential combination of both water oxidation and  $\text{CO}_2$  reduction. As these processes can be affected by parameters such as radiant flux intensity and the partial pressures of both  $\text{CO}_2$  and water vapour, these factors were systematically varied and studied in order to determine the most suitable process conditions for achieving high photocatalytic activity. Based on results from the  $\text{CO}_2$  photoreduction experiments, a total methane ( $\text{CH}_4$ ) yield of  $3.450 \mu\text{mol g}_{\text{cat}}^{-1}$  was successfully attained over 5GO-OTiO<sub>2</sub> after 8 h of reaction time under visible light irradiation. The experimental data obtained was then fitted into the Langmuir-Hinshelwood surface reaction mechanism, wherein both  $\text{CO}_2$  and  $\text{H}_2\text{O}$  adsorbed simultaneously on the photocatalyst surface to form the  $\text{CH}_4$  product. Regression fitting was performed to determine the kinetic parameters such as reaction rate constant and adsorption equilibrium constants. The reaction rate as well as  $\text{CO}_2$  and  $\text{H}_2\text{O}$  adsorption equilibrium constants were determined to be  $84.42 \mu\text{mol g}_{\text{cat}}^{-1} \text{h}^{-1}$ ,  $0.019 \text{bar}^{-1}$  and  $8.07 \text{bar}^{-1}$ , respectively. The significantly smaller  $\text{CO}_2$  adsorption equilibrium constant implied that the adsorption of  $\text{CO}_2$  was very weak while water strongly adsorbed on the photocatalyst surface.

**Keywords:** Graphene oxide, oxygen-rich, photocatalyst, carbon dioxide, process study, kinetics

## 1. Introduction

Fossil fuels are the major energy source used today and are rapidly consumed to meet the increasing energy demands of mankind. At the same time, carbon dioxide ( $\text{CO}_2$ ), an inevitable product of fossil fuel combustion, leads to possible climate change and result in serious impacts to the environment [1-5]. Therefore, the ability to harness the power of  $\text{CO}_2$  on a large scale and integrate it back into the utilization cycle as a sustainable form of energy production is highly desirable. Among the various renewable projects to date, the photocatalytic reduction of  $\text{CO}_2$  into energy-bearing products has garnered interdisciplinary research attention to mitigate the ever-growing  $\text{CO}_2$  concentration and to meet the long-term worldwide energy demands without utilizing further  $\text{CO}_2$ -generating power resources [6-15]. In this context, photocatalysis, a well-orchestrated mimic of natural photosynthesis, for direct conversion of solar energy to chemical energy, presents an opportunity to kill these two birds with one stone [16-19]. However, the state-of-the-art technology is far from being optimal due to low overall photoconversion and selectivity [20-22]. Hence, breakthroughs in the fabrication of highly efficient photocatalysts are necessary towards realizing the process for industrial applications.

Among the semiconductors that have been studied as photocatalysts for  $\text{CO}_2$  reduction, titanium dioxide ( $\text{TiO}_2$ ) is regarded as the most feasible in terms of its inexpensiveness, non-toxicity, high redox potentials and abundance [23-28]. Despite that, pure unmodified  $\text{TiO}_2$  suffers from several drawbacks such as low quantum efficiency resulting from rapid recombination of charge carriers and the limit to UV-light absorption due to its wide band gap [29-33]. Great endeavours have been made to resolve these drawbacks, including cationic metal and anionic doping to manipulate the properties of  $\text{TiO}_2$  [34-44]. However, these techniques could result in the generation of secondary impurities and oxygen vacancies, respectively, which could ultimately

reduce the photocatalytic activity of  $\text{TiO}_2$  [45, 46]. Under such circumstances, it becomes a necessity to develop an effective synthetic route to fabricate visible-light-responsive and stable  $\text{TiO}_2$  without the production of oxygen vacancies and secondary phases. In view of this, our research group has recently employed a dopant-free strategy to prepare a novel oxygen-rich  $\text{TiO}_2$  ( $\text{O}_2\text{-TiO}_2$ ) photocatalyst with significantly enhanced photocatalytic performance [47, 48]. By introducing oxygen excess defects into the lattice of  $\text{TiO}_2$ , the surface disorderliness caused an upshift of VB which led to a reduction of band gap energy from 3.2 eV to 2.95 eV. The resulting  $\text{O}_2\text{-TiO}_2$  could then be activated by visible light, generating electron-hole pairs on its surface. Although  $\text{O}_2\text{-TiO}_2$  showed remarkable efficiency in reducing  $\text{CO}_2$  into methane ( $\text{CH}_4$ ), its photocatalytic activity was observed to gradually deteriorate over time. This problem was successfully addressed by incorporating graphene oxide (GO) with  $\text{O}_2\text{-TiO}_2$  via a wet chemical impregnation technique [10]. In the graphene oxide/oxygen-rich  $\text{TiO}_2$  ( $\text{GO-OTiO}_2$ ) hybridized material, GO served as a sink for electrons and an effective charge transporting bridge owing to its high electron mobility and extended  $\pi$ -electron conjugation. The Schottky barrier formed at the interface of both components separated the photoinduced electron-hole pairs and decreased the charge recombination rate, which in turn improved the photostability of the hybrid composite significantly [10-12, 49, 50].

Our previous results showed that  $\text{GO-OTiO}_2$  with an optimum GO loading of 5 wt. % exhibited the highest photoactivity towards  $\text{CO}_2$  reduction. The total product yield obtained over  $\text{GO-OTiO}_2$  was found to be 14.0 folds higher in comparison to commercial Degussa P25 [10]. Nevertheless, the fundamental mechanism of photocatalytic  $\text{CO}_2$  reduction on  $\text{GO-OTiO}_2$  photocatalyst has yet to be explored so far. In overall, the  $\text{CO}_2$  conversion process is a sequential combination of both water oxidation and  $\text{CO}_2$  reduction [8, 20, 51, 52]. These processes can be

affected substantially under different experimental conditions such as the intensity and wavelength of the incident light, reactor configuration, residence time as well as the partial pressures of the reactants, *i.e.* CO<sub>2</sub> and water vapour [53-60]. Therefore, in the present work, parameters including incident light intensity as well as the partial pressures of CO<sub>2</sub> and water vapour were systematically varied and studied in order to determine their effects on the CO<sub>2</sub> photoreduction process. In heterogeneous photocatalytic processes, rates are typically proportional to the adsorption of reactant molecules with efficient desorption of products from the surface of the photocatalyst. When two reactants competitively adsorb on the same catalyst active sites, but with different adsorption and desorption rate constants, and undergoes reaction to yield different products, the reaction could be represented by the Langmuir-Hinshelwood (L-H) mechanism [53, 54, 61-65]. Hence, the L-H model was employed to correlate the as-obtained experimental data. Multiple variable, non-linear regression was carried out to determine the kinetic parameters such as reaction rate constant and adsorption equilibrium constants. The present work also aimed to extend the fundamental understanding of possible mechanism of CO<sub>2</sub> photoreduction over GO-OTiO<sub>2</sub> under visible light irradiation.

## 2. Experimental

### 2.1 Chemicals

Graphite powder (< 45 micron, > 99.99%), phosphorus pentoxide, P<sub>2</sub>O<sub>5</sub> (• 98.0%), potassium persulfate, K<sub>2</sub>S<sub>2</sub>O<sub>8</sub> (• 99.0%), potassium permanganate, KMnO<sub>4</sub> (• 99.0%), titanium (IV) butoxide, TBOT (97.0%), ethylene glycol, EG (• 99.0%), acetic acid, HAc (• 99.7%), Degussa P25 (21 nm particle size, • 99.5%) and anatase TiO<sub>2</sub> (< 25 nm particle size, 99.7%) were supplied by Sigma Aldrich. Hydrogen peroxide, H<sub>2</sub>O<sub>2</sub> (30.0%) and concentrated sulfuric acid, H<sub>2</sub>SO<sub>4</sub> (95-97%) were supplied by Chemolab. Hydrochloric acid, HCl (37% diluted to 10%) was supplied

by Merck. All chemicals were of analytical reagent grade and were used as received without further purification. Deionized water (DI-H<sub>2</sub>O) was used in all experiments.

## 2.2 Preparation of oxygen-rich TiO<sub>2</sub> (O<sub>2</sub>-TiO<sub>2</sub>) and graphene oxide/oxygen-rich TiO<sub>2</sub> (GO-OTiO<sub>2</sub>) hybrid composite.

The fabrication of O<sub>2</sub>-TiO<sub>2</sub> and GO-OTiO<sub>2</sub> has been reported in our previous work [10, 47, 48]. In brief, TBOT was added dropwise into pre-chilled DI-H<sub>2</sub>O, which resulted in an immediate precipitation of hydrolyzed titanium species. The solution was filtered and subsequently washed with 1 L of DI-H<sub>2</sub>O, after which the precipitate was added into a mixture consisting of 100 mL DI-H<sub>2</sub>O and 80 mL H<sub>2</sub>O<sub>2</sub>. The resulting orange colored peroxo-titanate complex was heated at 50 °C for 3 h, and then dried in an air oven at 100 °C overnight. The yellowish solid material was then calcined in air at 300 °C for 2 h with a temperature ramping rate of 10 °C/min. GO was incorporated with O<sub>2</sub>-TiO<sub>2</sub> *via* a wet chemical impregnation method. To attain GO sheets, graphite oxide powder was first synthesized using a modified Hummers' Method [66], followed by ultrasonication for 1.5 h to exfoliate and separate the graphitic layers. A pre-calculated amount of O<sub>2</sub>-TiO<sub>2</sub> powder was introduced into the GO aqueous solution and stirred for 1 h. The solution was heated to 80 °C for 2 h, and then dried in an air oven overnight before use. Based on our previous work [10], it was observed that GO-OTiO<sub>2</sub> with a GO loading of 5 wt. % (5GO-OTiO<sub>2</sub>) gave the optimum performance towards CO<sub>2</sub> photoreduction. Hence, the aforementioned photocatalyst was used throughout the present work.

## 2.3 Photocatalytic reduction of CO<sub>2</sub>

The schematic photocatalytic reaction system for the reduction of CO<sub>2</sub> with H<sub>2</sub>O in gaseous phase is shown in Fig. 1. The homemade photocatalytic system consisted of three quartz columns



connected in series, which were enclosed within a black box to avoid any interference from the surrounding light. The dimensions of the quartz columns are as follows: inner diameter = 9 mm, outer diameter = 11 mm, length = 250 mm. The entire system was checked for any leakages using a soap bubble solution. Process and kinetic studies of the CO<sub>2</sub> photoreduction process were conducted over 5GO-OTiO<sub>2</sub> photocatalyst. The sample was coated onto glass rods using double-sided tape, which were then loaded into the quartz columns. The photoreduction experiments were conducted at ambient condition ( $25 \pm 5$  °C, 1 bar) in a continuous gas flow reactor. A xenon arc lamp (Model no: CHF XM500W) with a UV cut-off filter ( $> 400$  nm) was employed throughout the study to focus the photocatalytic experiments solely on visible light irradiation. The average irradiance and light spectrum of the xenon lamp were recorded by an Avantes fiber optic spectrometer (AvaSpec-128) equipped with a cosine corrector. The required data was obtained using the AvaSoft-8 software. Before taking any measurements, an irradiance calibration was first carried out using the AvaLight-HAL-CAL light source. As an additional experiment, the photoreduction of CO<sub>2</sub> at optimized process conditions were repeated under the air mass 1.5 (AM1.5) filter. The light spectrums of the xenon arc lamp equipped with UV cut-off filter and the AM1.5 filter are shown in the Supplementary Material.

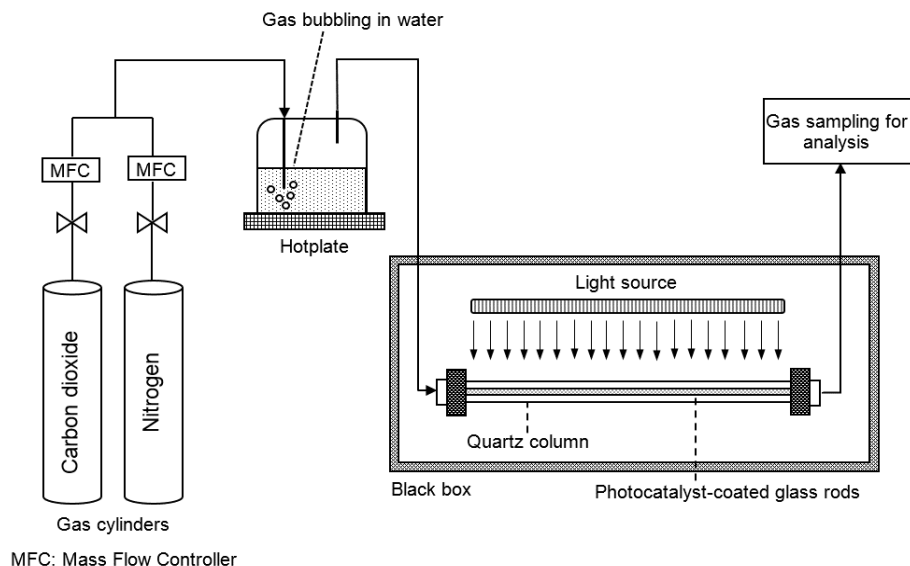


**Fig. 1.** Schematic of the apparatus used for the photocatalytic reduction of  $\text{CO}_2$  under visible light irradiation.

After loading the photocatalyst-coated glass rods, highly pure  $\text{CO}_2$  (99.99%) was bubbled through water to produce a mixture of  $\text{CO}_2$  and water vapour into the photoreactor at atmospheric pressure. Before switching on the light source, wet  $\text{CO}_2$  was permitted to flow through the photoreactor at 30 ml/min for 30 min to eliminate any excess air and to ensure the complete adsorption of gas molecules. After purging the reactor with wet  $\text{CO}_2$ , the xenon lamp was switched on and the flow of  $\text{CO}_2/\text{H}_2\text{O}$  was regulated using a mass flow controller. The temperature in the reactor was closely monitored with a thermocouple attached to a digital temperature reader. The distance between the light source and the photoreactor was measured to be about 5 cm. An “online” gas chromatography (GC) system (Agilent 7820A) coupled with flame ionization detector (FID) and thermal conductivity detector (TCD) was used to analyze the composition of the product gas. Throughout the fixed duration of 8 h, the product gas was collected and analyzed downstream of the reactor at 0.5 h intervals.

The process parameters studied in this work included the intensity of the incident light source as well as the partial pressures of both CO<sub>2</sub> and water vapour. To vary the intensity of the incident light, the electric current of the xenon arc lamp was manipulated in the range of 5 – 15 A, where the irradiance (mW/cm<sup>2</sup>) at each setting was recorded (see Supplementary Material). The partial pressure of CO<sub>2</sub>, P<sub>CO<sub>2</sub></sub> used in the photocatalytic experiment was varied in the range of 25 – 101 kPa, which was achieved by controlling the flow ratio of CO<sub>2</sub> to the inert gas N<sub>2</sub>. The total flow rate entering the photoreactor was held constant at 5 ml/min throughout the duration of all experiments. Finally, the partial pressure of H<sub>2</sub>O, P<sub>H<sub>2</sub>O</sub> or moisture content entering the photoreactor was varied by controlling the temperature of the water saturator.

### **3. Results and Discussion**

#### **3.1 Effects of process parameters on the photoreduction of CO<sub>2</sub> under visible light irradiation**

Initially, a series of control experiments were performed to confirm that the hydrocarbon products were generated through photocatalytic reaction rather than through organic decomposition of the 5GO-OTiO<sub>2</sub> photocatalyst. The control experiments were conducted under the following conditions: (1) in the dark (without light irradiation) with the presence of photocatalyst and CO<sub>2</sub>/H<sub>2</sub>O flow, (2) without photocatalyst under CO<sub>2</sub>/H<sub>2</sub>O flow and light irradiation, (3) in the absence of H<sub>2</sub>O vapor with photocatalyst, CO<sub>2</sub> flow and light irradiation and (4) under N<sub>2</sub>/H<sub>2</sub>O atmosphere in the presence of photocatalyst and light irradiation. In all cases, no appreciable product formation could be detected. This confirmed that the evolved products were generated through the photocatalytic process and not from the photodecomposition of organic residues on the catalyst. Therefore, it can be reiterated that the

CO<sub>2</sub> photoreduction process required all three components, *i.e.* the presence of photocatalysts, reactant feed (CO<sub>2</sub> and H<sub>2</sub>O) and light irradiation.

The intensity of the light source was varied between 65.3 – 177.2 mW/cm<sup>2</sup> (see Supplementary Material). The CO<sub>2</sub> photoreduction experiments were conducted at a fixed CO<sub>2</sub> flowrate of 5 ml/min at ambient condition. The temperature of the photocatalytic system was closely monitored throughout the duration of the reaction. Despite the high intensity of the xenon arc lamp used in the experiments, the temperature increase was observed to be minimal and insignificant. Fig. 2(a) shows the total CH<sub>4</sub> yield versus light intensity under fixed CO<sub>2</sub> and H<sub>2</sub>O pressures of 101 and 4.33 kPa, respectively. The total CH<sub>4</sub> yield attained was promoted almost linearly with the incident light intensity. At an intensity of 177.2 mW/cm<sup>2</sup>, the highest total CH<sub>4</sub> yield of 3.14 μmol g<sub>cat</sub><sup>-1</sup> was achieved after 8 h of light irradiation. This observation could be attributed to the large number of photons striking the surface of the 5GO-OTiO<sub>2</sub> photocatalyst, which in turn powered the excitation of more electrons and holes to take part in the photoreduction of CO<sub>2</sub> into CH<sub>4</sub> gas [67-69].

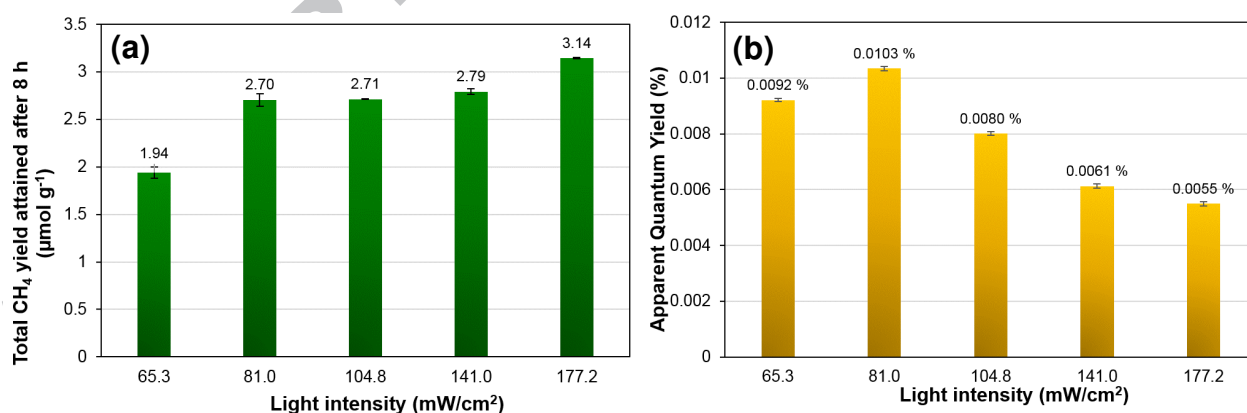


**Fig. 2.** (a) Total methane yield and (b) apparent quantum yield attained over 5GO-OTiO<sub>2</sub> after 8 h at different light intensities, P<sub>CO<sub>2</sub></sub> : 101 kPa; P<sub>H<sub>2</sub>O</sub> : 4.33 kPa.

Although the photocatalytic performance of a sample is typically measured by the product yield attained in terms of  $\mu\text{mol g}_{\text{cat}}^{-1}$  or  $\mu\text{mol g}_{\text{cat}}^{-1} \text{h}^{-1}$ , it should be noted that the photocatalytic activity is generally dependent on other factors such as the intensity of the light source employed. Therefore, to determine the optimum light intensity for this process, the apparent quantum yield (AQY) was adopted. AQY is defined as the ratio of the number of electrons reacted to the number of incident photons at that time period. The general equation is described by Eq. (1). In the photocatalytic reduction of  $\text{CO}_2$  into  $\text{CH}_4$  gas, eight electrons are consumed per formation of one  $\text{CH}_4$  molecule as described by Eq. (2). Hence, the number of electrons reacted can be directly calculated by multiplying the number of  $\text{CH}_4$  molecules evolved by eight. As a result, the AQY can be estimated by Eq. (3) [49, 70].

$$\text{Apparent quantum yield}(\%) = \frac{\text{Number of reacted electrons}}{\text{Number of incident photons}} \times 100\% \quad (1)$$



$$\text{Apparent quantum yield}(\%) = \frac{[\text{CH}_4] \times 8 \times N_A}{H \times A \times \frac{\lambda}{hc} \times t} \times 100\% \quad (3)$$

Where  $[\text{CH}_4]$  represents the amount of  $\text{CH}_4$  evolved during the photoreaction (mol),  $N_A$  is the Avogadro's number ( $\text{mol}^{-1}$ ),  $H$  is the apparent light intensity used ( $\text{W m}^{-2}$ ),  $A$  is the irradiation area ( $\text{m}^2$ ),  $\lambda$  is the light wavelength (m),  $h$  is the Planck's constant (J s),  $c$  is the speed of light ( $\text{m s}^{-1}$ ) and  $t$  is the reaction time (s).

The AQY obtained over 5GO-OTiO<sub>2</sub> photocatalyst at different light intensities are shown in Fig. 2(b). Among the studied incident light intensities, 5GO-OTiO<sub>2</sub> was observed to exhibit the highest AQY of 0.0103% at an intensity of 81.0 mW/cm<sup>2</sup>. An optimum value existed because at

excessively high light intensities ( $> 81 \text{ mW/cm}^2$ ), the photons supplied to the photocatalyst would have exceeded the number of photons required for the photocatalytic reaction. Therefore, an irradiance of  $81 \text{ mW/cm}^2$  gave the most efficient utilization of photon energy and was hence used in all subsequent studies.

The influence of  $\text{CO}_2$  partial pressure on the photocatalytic activity was also investigated. As the present work focuses mainly on the production of hydrocarbon fuels, the representation of photocatalytic efficiency was directed towards the total yield of  $\text{CH}_4$  product. Fig. 3(a) shows the total  $\text{CH}_4$  yields attained over  $5\text{GO-OTiO}_2$  after 8 h versus different  $\text{CO}_2$  pressures under fixed light intensity,  $81 \text{ mW/cm}^2$  and water pressure,  $4.33 \text{ kPa}$  at room temperature. From Fig. 3(a), it can be observed that the total yield of  $\text{CH}_4$  increased with  $P_{\text{CO}_2}$ , where it reached a maximum value of  $3.08 \mu\text{mol g}_{\text{cat}}^{-1}$  at  $90 \text{ kPa}$ , before decreasing with a further increment of  $P_{\text{CO}_2}$ . This phenomenon was likely due to the competitive adsorption between  $\text{CO}_2$  and  $\text{H}_2\text{O}$  molecules on the active sites of  $5\text{GO-OTiO}_2$  during the photoreduction process. At lower concentrations of  $\text{CO}_2$ , a large amount of  $\text{H}_2\text{O}$  molecules could have adsorbed on the photocatalyst surface to react with a limited number of  $\text{CO}_2$  molecules to form  $\text{CH}_4$ . On the other hand, at excessively high  $\text{CO}_2$  concentrations, the  $\text{CO}_2$  molecules would compete with  $\text{H}_2\text{O}$  molecules for the active sites, leading to poor overall photoactivity [61, 65, 71]. Therefore, an optimum concentration of both reactants exists for achieving high  $\text{CH}_4$  yield. A similar trend of results have also been reported by other research groups [57, 61, 65].

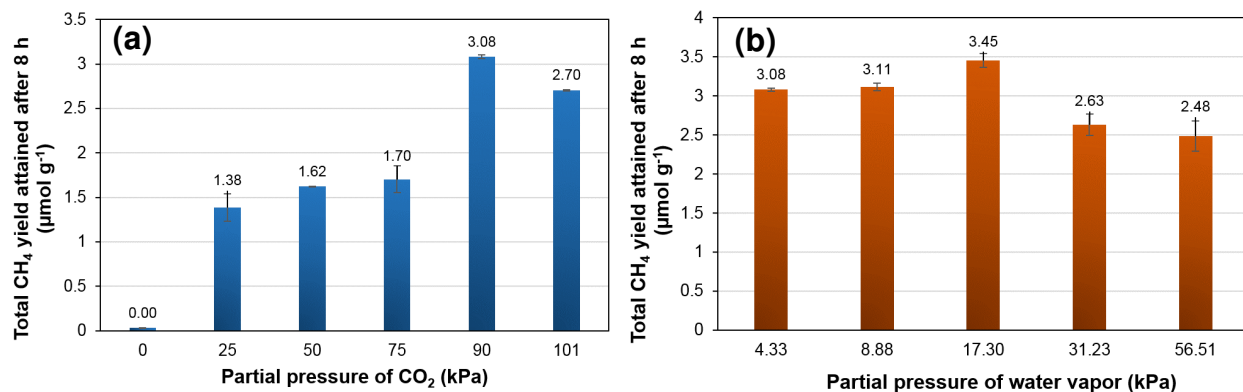


**Fig. 3.** Total methane yield attained over 5GO-OTiO<sub>2</sub> after 8 h at (a) different partial pressures of CO<sub>2</sub>, light intensity: 81.0 mW/cm<sup>2</sup>; P<sub>H<sub>2</sub>O</sub>: 4.33 kPa; and at (b) different partial pressures of H<sub>2</sub>O, light intensity: 81.0 mW/cm<sup>2</sup>; P<sub>CO<sub>2</sub></sub>: 90 kPa.

Fig. 3(b) illustrates the effect of H<sub>2</sub>O partial pressure on the photocatalytic activity of 5GO-OTiO<sub>2</sub>, under fixed light intensity and CO<sub>2</sub> pressure of 81 mW/cm<sup>2</sup> and 90 kPa, respectively. From Fig. 3(b), the total CH<sub>4</sub> yield can be seen to have increased with P<sub>H<sub>2</sub>O</sub> until reaching a maximum value of 3.45 μmol g<sub>cat</sub><sup>-1</sup> at 17.3 kPa. Increasing the P<sub>H<sub>2</sub>O</sub> further was found to have a negative impact on the photocatalytic performance of 5GO-OTiO<sub>2</sub>. Similar to the case of P<sub>CO<sub>2</sub></sub>, this phenomenon implied a competitive adsorption of reactants, *i.e.* CO<sub>2</sub> and H<sub>2</sub>O for the active sites during the photoreduction process [61]. The presence of water vapour in the CO<sub>2</sub> photoreduction process is indispensable due to its role in producing certain reactive intermediate radicals. During the photocatalytic reduction of CO<sub>2</sub>, the photogenerated holes (h<sup>+</sup>) react with H<sub>2</sub>O to yield H<sup>+</sup> ions and •OH radicals, both of which are required for the subsequent reduction of CO<sub>2</sub>. The •H radicals which originate from the reduction of protons, will react with carbon radicals on the photocatalyst surface to produce methyl radicals, *i.e.* •CH<sub>2</sub>, •CH<sub>3</sub> and finally CH<sub>4</sub> as well as higher hydrocarbons *e.g.* C<sub>2</sub>H<sub>4</sub> and C<sub>2</sub>H<sub>6</sub> [53, 57, 72]. Therefore, H<sub>2</sub>O is needed in appropriate concentrations to ensure the sufficient supply of H<sup>+</sup> ions and •OH for the formation of

these hydrocarbon products. However, excessively high H<sub>2</sub>O concentrations would occupy the catalyst active sites and consequently reduce the surface contact of CO<sub>2</sub> molecules with the photocatalyst.

The highest CH<sub>4</sub> yield of 3.45 μmol g<sub>cat</sub><sup>-1</sup> could be obtained over 5GO-OTiO<sub>2</sub> at P<sub>CO<sub>2</sub></sub> = 90 kPa, P<sub>H<sub>2</sub>O</sub> = 17.3 kPa under an incident visible light intensity of 81.0 mW/cm<sup>2</sup> after 8 h. In addition to CH<sub>4</sub>, other products such as CO, C<sub>2</sub>H<sub>4</sub> and C<sub>2</sub>H<sub>6</sub> were also detected at the outlet gas (see Fig. 4). The total yield of CO evolved was found to be approximately 2.6 times higher than that of CH<sub>4</sub>. This observation could be explained based on the energy band theory. Principally, photoexcited electrons could only be consumed effectively if the reduction potential of the reaction is lower than the CB potential of the semiconductor. In this case, the 5GO-OTiO<sub>2</sub> photocatalyst was more feasible in driving the reduction of CO<sub>2</sub> into CO because of the lower reduction potential difference of (E°(CO<sub>2</sub>/CO = -0.53V) as compared to CH<sub>4</sub> (E°(CO<sub>2</sub>/CH<sub>4</sub> = -0.24V) [73]. Therefore, in the continuous process, a significant amount of CO was produced.

In an additional experiment, the photocatalytic reduction of CO<sub>2</sub> at optimized process conditions was repeated under the air mass 1.5 (AM1.5) filter (see Fig. 4). The use of the AM1.5 provides one of the best options for simulating natural sunlight [74]. It was found that the total yield of all four products was higher under the AM1.5 filter than that of UV cut-off. This is because UV-light is generally known to exhibit higher energy per photon, which has the potential to effectively power the excitation of more electrons and holes for the photocatalytic reactions, thus leading to the increase in product yield [75]. To confirm the as-obtained results, the CO<sub>2</sub> photoreduction experiment conducted under the optimized process conditions were repeated. The



standard error for the formation of each product was found to be approximately  $\pm 0.1$ , thus confirming the reproducibility of the results.

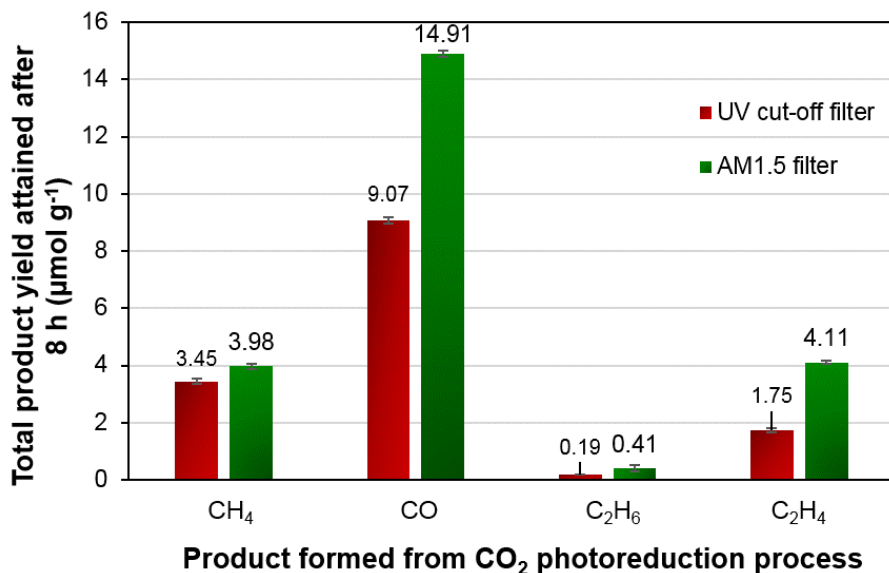


**Fig. 4.** Total yield of CH<sub>4</sub>, CO, C<sub>2</sub>H<sub>6</sub> and C<sub>2</sub>H<sub>4</sub> attained over 5GO-OTiO<sub>2</sub> after 8 h under different light filters.

### 3.2 Kinetic study of the photocatalytic reduction of CO<sub>2</sub> over 5GO-OTiO<sub>2</sub> composite

In heterogeneous photocatalytic processes, rates are typically proportional to the adsorption of reactants with efficient desorption of products on the photocatalyst surface. When two reactants competitively adsorb on the same catalyst surface active sites, but with different adsorption and desorption constants, the reaction can be represented using the Langmuir-Hinshelwood mechanism [76], as described by Eq. (4).

$$\text{Rate} = k\theta_A\theta_B = k \frac{K_A P_A K_B P_B}{(1 + K_A P_A + K_B P_B)^2}$$

(4)

Where  $\theta_A$  and  $\theta_B$  represent the fractional surface coverage of each reactant, while  $P_A$  and  $P_B$  are the partial pressures of each reactant species. The rate constant,  $k$  and adsorption equilibrium constants,  $K_A$  and  $K_B$ , are dependent on the system temperature. If the adsorption is random, the adsorption probability would be taken as the fraction of the uncovered surface ( $1 - \theta$ ), while desorption would be taken as the surface covered,  $\theta$ . By employing these assumptions, the kinetic model for the photocatalytic reduction of  $\text{CO}_2$  with  $\text{H}_2\text{O}$  could be developed. In the photoreduction process,  $\text{CO}_2$  and  $\text{H}_2\text{O}$  were photocatalytically converted into  $\text{CH}_4$  and  $\text{CO}$  as main products through Eq. (5).



There are five primary steps in the photocatalytic reaction mechanism. Step 1 is the adsorption of reactants, *i.e.*  $\text{CO}_2$  and  $\text{H}_2\text{O}$  onto the active sites of  $5\text{GO-OTiO}_2$ ; Step 2 consists of light absorption and subsequent production of photoinduced electrons and holes on the photocatalyst surface; Step 3 is the interaction between the charge carriers and adsorbed reactant molecules, as well as the recombination of charge particles; Step 4 consists of both the oxidation and reduction reactions while the last step is the desorption of products from the photocatalyst surface [53, 65]. Among the aforementioned steps, the surface reaction is typically considered to be the slowest and hence the rate determining step (RDS) [53, 54]. By assuming the reactants and products are adsorbed on the same catalyst surface active sites, the rate of reaction in the  $\text{CO}_2$  photoreduction process can be explained by the Langmuir-Hinshelwood mechanism as described in Eq. (6).

$$\text{Rate} = (kI^a) \left( \frac{K_{\text{H}_2\text{O}} P_{\text{H}_2\text{O}} K_{\text{CO}_2} P_{\text{CO}_2}}{(1 + K_{\text{H}_2\text{O}} P_{\text{H}_2\text{O}} + K_{\text{CO}_2} P_{\text{CO}_2} + K_{\text{CO}} P_{\text{CO}} + K_{\text{O}_2} P_{\text{O}_2} + K_{\text{CH}_4} P_{\text{CH}_4})^2} \right)$$

(6)

Where  $k$  represents the rate constant of any particular product and  $I$  is the incident light intensity in which the kinetic constants are evaluated. Generally, the photocatalytic reaction rate is proportional to  $I^a$ , where  $a$  is the reaction order of the light intensity.  $K_{H_2O}$ ,  $K_{CO_2}$ ,  $K_{CO}$ ,  $K_{O_2}$  and  $K_{CH_4}$  are the ratios of rate constants for adsorption and desorption of  $H_2O$ ,  $CO_2$ ,  $CO$ ,  $O_2$  and  $CH_4$ , respectively. By assuming that only reactants are adsorbed onto the photocatalyst surface while all products desorbed immediately after chemical reaction, Eq. (6) can be further simplified to Eq. (7). In addition, the reaction was considered to be irreversible because the partial pressures of the products were very low [61].

$$\text{Rate} = (kI^a K_{H_2O} K_{CO_2}) \left( \frac{P_{H_2O} P_{CO_2}}{(1 + K_{H_2O} P_{H_2O} + K_{CO_2} P_{CO_2})^2} \right) \quad (7)$$

The constants of the L-H model were solved by correlating it with the experimental data of  $P_{CO_2}$ ,  $P_{H_2O}$ , light intensity and the  $CH_4$  production rate obtained from Section 3.1, where the light intensity,  $I$  was fixed at the optimum value of  $81.0 \text{ mW/cm}^2$ . Multiple-variable non-linear regression was performed using Polymath software, version 6.10. The best fitted rate constant,  $k$ , adsorption equilibrium constants,  $K_{H_2O}$  and  $K_{CO_2}$  as well as the reaction order of the light intensity,  $a$  are tabulated in Table 1. The fitted model showed high degree of precision, exhibiting an R-squared value of 0.922 with small sums of squares/ variance. By incorporating the values of the kinetic constants, the resulting rate model for the photocatalytic reduction of  $CO_2$  over 5GO-OTiO<sub>2</sub> is presented in Eq. (8).

**Table 1.** Adsorption equilibrium and rate constants of Langmuir-Hinshelwood model estimated using experimental data on 5GO-OTiO<sub>2</sub>.

Parameter	Value	Error with 95% confidence
Reaction rate constant, k ( $\mu\text{mol g}_{\text{cat}}^{-1} \text{h}^{-1}$ )	84.42	$\pm 0.267$
Reaction order of light intensity, <i>a</i>	0.044	$\pm 0.0007$
Adsorption equilibrium of H <sub>2</sub> O, <i>K</i> <sub>H<sub>2</sub>O</sub> (bar <sup>-1</sup> )	8.070	$\pm 0.0620$
Adsorption equilibrium of CO <sub>2</sub> , <i>K</i> <sub>CO<sub>2</sub></sub> (bar <sup>-1</sup> )	0.0193	$\pm 0.0001$

$$\text{Rate} = 15.953 \left( \frac{P_{\text{H}_2\text{O}} P_{\text{CO}_2}}{(1 + 8.070 P_{\text{H}_2\text{O}} + 0.0193 P_{\text{CO}_2})^2} \right) \quad (8)$$

Based on the tabulated data in Table 1, the value of H<sub>2</sub>O adsorption equilibrium, *K*<sub>H<sub>2</sub>O</sub> was 8.07 bar<sup>-1</sup>, which was significantly higher than that of CO<sub>2</sub> (*K*<sub>CO<sub>2</sub></sub> = 0.02 bar<sup>-1</sup>). The value of *K*<sub>CO<sub>2</sub></sub> was near zero, which directly indicated very weak adsorption of CO<sub>2</sub> molecules, while water was strongly adsorbed on the surface of the 5GO-OTiO<sub>2</sub> photocatalyst. This is because, in addition to the strong hydrophilic nature of graphene oxide [77, 78]. it is well known that the surface of TiO<sub>2</sub>

becomes superhydrophilic when irradiated by light [79]. Therefore, water would wet most of the surface of 5GO-OTiO<sub>2</sub> during the photocatalytic process. As shown in Table 1, the power of the light intensity was estimated to be approximately 0.044 in the CH<sub>4</sub> rate equation. As discussed earlier, photocatalytic activity is generally directly proportional to the light intensity. However, if the supply of light flux exceeds the demand for the photoreaction, the power of light intensity in the rate equation would gradually shift from one to less than 0.5. Therefore, it can be deduced that the light flux used in our experiments was probably over-supplied and can be decreased to enhance the quantum efficiency of the photocatalytic system. To prove the validity of the rate model in Eq. (8), the CO<sub>2</sub> photoreduction experiments were repeated and the production rate of CH<sub>4</sub> were compared to that obtained from the rate model. The curves representing the profiles of CH<sub>4</sub> production rate as a function of  $P_{H_2O}$  and  $P_{CO_2}$  using the kinetic model is shown in the Supplementary Material. The model was shown to have fitted well to the experimental data using the constants as summarized in Table 1, with R<sup>2</sup> values above 0.95.

Although the detailed mechanism underlying the formation of CH<sub>4</sub> could not be determined in the present study, a CO<sub>2</sub> photoreduction mechanism is suggested based on the L-H model derived and is illustrated in Fig. 5. The photocatalytic process begins with the adsorption of reactant molecules, *i.e.* CO<sub>2</sub> and H<sub>2</sub>O molecules onto the surface of 5GO-OTiO<sub>2</sub>. In the surface reaction step, photogenerated electrons are transferred to the adsorbed CO<sub>2</sub> to yield •CO<sub>2</sub><sup>-</sup> radicals. The holes, on the other hand, react with adsorbed H<sub>2</sub>O molecules to produce H<sup>+</sup> ions and •OH radicals, and subsequently O<sub>2</sub> [80]. The •H radicals formed through the reduction of proton then react with carbon radicals on the photocatalyst surface to yield intermediate radicals and the hydrocarbon products. All possible reaction steps which take place in the photocatalytic reduction of CO<sub>2</sub> with

H<sub>2</sub>O are explained by Eq. (9 – 13). Desorption of the evolved products represents the final step in the photocatalytic process.

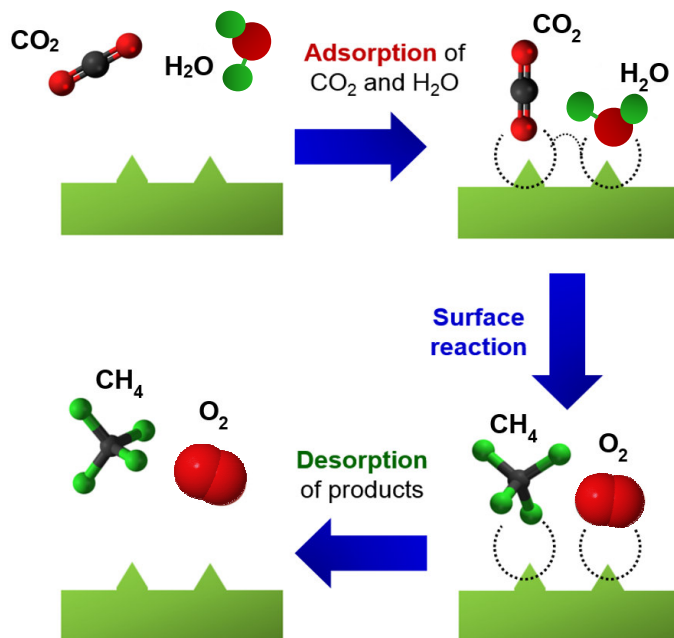
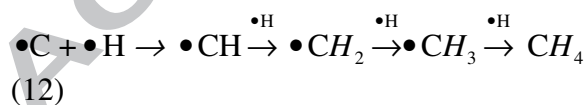


**Fig. 5.** Conceptual diagram depicting the reaction mechanism of the CO<sub>2</sub> photoreduction process based on the Langmuir-Hinshelwood mechanism.



#### 4. Conclusions

In summary, process parameters including radiant flux intensity and the partial pressures of both CO<sub>2</sub> and water vapour were systematically varied and studied in order to study their effects on the CO<sub>2</sub> photoreduction process over 5GO-OTiO<sub>2</sub> photocatalyst. The visible light irradiance was varied between 65.3 to 177.2 mW/cm<sup>2</sup> to study its effect on the apparent quantum yield (AQY) of 5GO-OTiO<sub>2</sub>. It was found that the optimum irradiance for the process was 80.97 mW/cm<sup>2</sup>. Beyond that value, the AQY was shown to have gradually decreased. This was because the photons generated at excessively high light intensities have exceeded the number of photons required for the photocatalytic reaction. The partial pressure of CO<sub>2</sub> and water vapour which gave the highest yield of CH<sub>4</sub> gas was found to be 90 kPa and 17.3 kPa, respectively. The combination of these process parameters resulted in a total CH<sub>4</sub> yield of 3.450 μmol g<sub>cat</sub><sup>-1</sup> after 8 h of reaction time. The experimental data obtained was then fitted into the Langmuir-Hinshelwood surface reaction mechanism, wherein both CO<sub>2</sub> and H<sub>2</sub>O adsorbed simultaneously on the photocatalyst surface to form the CH<sub>4</sub> product. Through regression fitting, the reaction rate as well as CO<sub>2</sub> and H<sub>2</sub>O adsorption equilibrium constants were determined to be 84.42 μmol g<sub>cat</sub><sup>-1</sup> h<sup>-1</sup>, 0.019 bar<sup>-1</sup> and 8.07 bar<sup>-1</sup>, respectively. The significantly smaller CO<sub>2</sub> adsorption equilibrium constant implied that the adsorption of CO<sub>2</sub> was very weak while water strongly adsorbed on the photocatalyst surface. The fitted model showed high degree of precision, exhibiting an R-squared value of 0.95.

#### Acknowledgements

This work was funded by the Ministry of Science, Technology and Innovation (MOSTI) Malaysia and the Ministry of Higher Education (MOHE) under e-Science Fund (Ref.

no. 03-02-10-SF0244) and the Fundamental Research Grant Scheme (FRGS) (Ref. no. FRGS/1/2013/TK05/MUSM/02/1), respectively.

## References

- [1] S.I. Seneviratne, M.G. Donat, A.J. Pitman, R. Knutti, R.L. Wilby, Allowable CO<sub>2</sub> emissions based on regional and impact-related climate targets, *Nature* 529 (2016) 477-483.
- [2] M. Forkel, N. Carvalhais, C. Rödenbeck, R. Keeling, M. Heimann, K. Thonicke, S. Zaehle, M. Reichstein, Enhanced seasonal CO<sub>2</sub> exchange caused by amplified plant productivity in northern ecosystems, *Science* DOI: 10.1126/science.aac4971 (2016).
- [3] J. Chang, P. Ciais, N. Viovy, N. Vuichard, M. Herrero, P. Havlík, X. Wang, B. Sultan, J.-F. Soussana, Effect of climate change, CO<sub>2</sub> trends, nitrogen addition, and land-cover and management intensity changes on the carbon balance of European grasslands, *Global Change Biology* 22 (2016) 338-350.
- [4] H. Kashiwagi, Atmospheric carbon dioxide and climate change since the Late Jurassic (150 Ma) derived from a global carbon cycle model, *Palaeogeography, Palaeoclimatology, Palaeoecology* 454 (2016) 82-90.
- [5] Y. Hao, H. Chen, Y.-M. Wei, Y.-M. Li, The influence of climate change on CO<sub>2</sub> (carbon dioxide) emissions : an empirical estimation based on Chinese provincial panel data, *J. Clean. Prod.* DOI: 10.1016/j.jclepro.2016.04.117.
- [6] A. Sarkar, E. Gracia-Espino, T. Wågberg, A. Shchukarev, M. Mohl, A.-R. Rautio, O. Pitkänen, T. Sharifi, K. Kordas, J.-P. Mikkola, Photocatalytic reduction of CO<sub>2</sub> with H<sub>2</sub>O over modified TiO<sub>2</sub> nanofibers: Understanding the reduction pathway, *Nano Res.* DOI: 10.1007/s12274-016-1087-9 (2016) 1-13.



- [7] J.-C. Wang, H.-C. Yao, Z.-Y. Fan, L. Zhang, J.-S. Wang, S.-Q. Zang, Z.-J. Li, Indirect Z-Scheme BiOI/g-C<sub>3</sub>N<sub>4</sub> photocatalysts with enhanced photoreduction CO<sub>2</sub> activity under visible light irradiation, *ACS Appl. Mater. Interfaces* 8 (2016) 3765-3775.
- [8] X. Chang, T. Wang, J. Gong, CO<sub>2</sub> photo-reduction: insights into CO<sub>2</sub> activation and reaction on surfaces of photocatalysts, *Energy Environ. Sci.* DOI: 10.1039/C6EE00383D (2016).
- [9] B. Yu, Y. Zhou, P. Li, W. Tu, P. Li, L. Tang, J. Ye, Z. Zou, Photocatalytic reduction of CO<sub>2</sub> over Ag/TiO<sub>2</sub> nanocomposites prepared with a simple and rapid silver mirror method, *Nanoscale* DOI: 10.1039/C6NR02547A (2016).
- [10] L.-L. Tan, W.-J. Ong, S.-P. Chai, B.T. Goh, A.R. Mohamed, Visible-light-active oxygen-rich TiO<sub>2</sub> decorated 2D graphene oxide with enhanced photocatalytic activity toward carbon dioxide reduction, *Appl. Catal., B* 179 (2015) 160-170.
- [11] L.-L. Tan, W.-J. Ong, S.-P. Chai, A.R. Mohamed, Reduced graphene oxide-TiO<sub>2</sub> nanocomposite as a promising visible-light-active photocatalyst for the conversion of carbon dioxide, *Nanoscale Res. Lett.* 8 (2013) 465-473.
- [12] L.-L. Tan, W.-J. Ong, S.-P. Chai, A.R. Mohamed, Noble metal modified reduced graphene oxide/TiO<sub>2</sub> ternary nanostructures for efficient visible-light-driven photoreduction of carbon dioxide into methane, *Appl. Catal., B* 166–167 (2015) 251-259.
- [13] W.-J. Ong, L.-L. Tan, S.-P. Chai, S.-T. Yong, A.R. Mohamed, Surface charge modification via protonation of graphitic carbon nitride (g-C<sub>3</sub>N<sub>4</sub>) for electrostatic self-assembly construction of 2D/2D reduced graphene oxide (rGO)/g-C<sub>3</sub>N<sub>4</sub> nanostructures toward enhanced photocatalytic reduction of carbon dioxide to methane, *Nano Energy* 13 (2015) 757-770.

- [14] H.-Q. Xu, J. Hu, D. Wang, Z. Li, Q. Zhang, Y. Luo, S.-H. Yu, H.-L. Jiang, Visible-light photoreduction of CO<sub>2</sub> in a metal–organic framework: Boosting electron–hole separation via electron trap states, *J. Am. Chem. Soc.* 137 (2015) 13440-13443.
- [15] M.-Q. Yang, N. Zhang, M. Pagliaro, Y.-J. Xu, Artificial photosynthesis over graphene-semiconductor composites. Are we getting better?, *Chem. Soc. Rev.* 43 (2014) 8240-8254.
- [16] W.-J. Ong, L.-L. Tan, Y.H. Ng, S.-T. Yong, S.-P. Chai, Graphitic carbon nitride (g-C<sub>3</sub>N<sub>4</sub>)-based photocatalysts for artificial photosynthesis and environmental remediation: Are we a step closer to achieving sustainability?, *Chem. Rev.* DOI: 10.1021/acs.chemrev.6b00075 (2016).
- [17] L.K. Putri, L.-L. Tan, W.-J. Ong, W.S. Chang, S.-P. Chai, Graphene oxide: Exploiting its unique properties toward visible-light-driven photocatalysis, *Appl. Mater. Today* 4 (2016) 9-16.
- [18] O. Ola, M.M. Maroto-Valer, Review of material design and reactor engineering on TiO<sub>2</sub> photocatalysis for CO<sub>2</sub> reduction, *J. Photochem. Photobiol., C* 24 (2015) 16-42.
- [19] P. Zhou, J. Yu, M. Jaroniec, All-solid-state Z-scheme photocatalytic systems, *Adv. Mater.* 26 (2014) 4920-4935.
- [20] A.D. Handoko, K. Li, J. Tang, Recent progress in artificial photosynthesis: CO<sub>2</sub> photoreduction to valuable chemicals in a heterogeneous system, *Curr. Opin. Chem. Eng.* 2 (2013) 200-206.
- [21] K. Li, X. An, K.H. Park, M. Khraisheh, J. Tang, A critical review of CO<sub>2</sub> photoconversion: Catalysts and reactors, *Catal. Today* 224 (2014) 3-12.
- [22] J.L. White, M.F. Baruch, J.E. Pander Iii, Y. Hu, I.C. Fortmeyer, J.E. Park, T. Zhang, K. Liao, J. Gu, Y. Yan, T.W. Shaw, E. Abelev, A.B. Bocarsly, Light-driven heterogeneous

- reduction of carbon dioxide: Photocatalysts and photoelectrodes, *Chem. Rev.* 115 (2015) 12888-12935.
- [23] W.-J. Ong, L.-L. Tan, S.-P. Chai, S.-T. Yong, A.R. Mohamed, Highly reactive {001} facets of TiO<sub>2</sub>-based composites: synthesis, formation mechanism and characterization, *Nanoscale* 6 (2014) 1946-2008.
- [24] W.-J. Ong, L.-L. Tan, S.-P. Chai, S.-T. Yong, A.R. Mohamed, Facet-dependent photocatalytic properties of TiO<sub>2</sub>-based composites for energy conversion and environmental remediation, *ChemSusChem* 7 (2014) 690-719.
- [25] P. Pichat, Fundamentals of TiO<sub>2</sub> Photocatalysis. Consequences for Some Environmental Applications, in: C.J. Colmenares, Y.-J. Xu (Eds.) *Heterogeneous Photocatalysis: From Fundamentals to Green Applications*, Springer Berlin Heidelberg, Berlin, Heidelberg, 2016, pp. 321-359.
- [26] C. Peng, X. Yang, Y. Li, H. Yu, H. Wang, F. Peng, Hybrids of two-dimensional Ti<sub>3</sub>C<sub>2</sub> and TiO<sub>2</sub> Exposing {001} facets toward enhanced photocatalytic activity, *ACS Appl. Mater. Interfaces* 8 (2016) 6051-6060.
- [27] G. Peng, J.E. Ellis, G. Xu, X. Xu, A. Star, In situ grown TiO<sub>2</sub> nanospindles facilitate the formation of holey reduced graphene oxide by photodegradation, *ACS Appl. Mater. Interfaces* 8 (2016) 7403-7410.
- [28] X. Liu, G. Dong, S. Li, G. Lu, Y. Bi, Direct observation of charge separation on anatase TiO<sub>2</sub> crystals with selectively etched {001} facets, *J. Am. Chem. Soc.* 138 (2016) 2917-2920.
- [29] S.J. Pearton, C.R. Abernathy, M.E. Overberg, G.T. Thaler, D.P. Norton, N. Theodoropoulou, A.F. Hebard, Y.D. Park, F. Ren, J. Kim, L.A. Boatner, Wide band gap ferromagnetic semiconductors and oxides, *J. Appl. Phys.* 93 (2003) 1-13.

- [30] N. Serpone, Is the band gap of pristine TiO<sub>2</sub> narrowed by anion- and cation-doping of titanium dioxide in second-generation photocatalysts?, *J. Phys. Chem. B* 110 (2006) 24287-24293.
- [31] S. Mubeen, G. Hernandez-Sosa, D. Moses, J. Lee, M. Moskovits, Plasmonic photosensitization of a wide band gap semiconductor: Converting plasmons to charge carriers, *Nano Lett.* 11 (2011) 5548-5552.
- [32] J.B. Varley, A. Janotti, C. Franchini, C.G. Van de Walle, Role of self-trapping in luminescence and p-type conductivity of wide-band-gap oxides, *Phys. Rev. B* 85 (2012) 081109.
- [33] H. Yan, X. Wang, M. Yao, X. Yao, Band structure design of semiconductors for enhanced photocatalytic activity: The case of TiO<sub>2</sub>, *Progress in Natural Science: Materials International* 23 (2013) 402-407.
- [34] D. Zhao, C. Chen, Y. Wang, H. Ji, W. Ma, L. Zang, J. Zhao, Surface modification of TiO<sub>2</sub> by phosphate: Effect on photocatalytic activity and mechanism implication, *J. Phys. Chem. C* 112 (2008) 5993-6001.
- [35] M.G. Méndez-Medrano, E. Kowalska, A. Lehoux, A. Herissan, B. Ohtani, D. Bahena, V. Briois, C. Colbeau-Justin, J.L. Rodríguez-López, H. Remita, Surface modification of TiO<sub>2</sub> with Ag nanoparticles and CuO nanoclusters for application in photocatalysis, *J. Phys. Chem. C* 120 (2016) 5143-5154.
- [36] M. Epifani, R. Díaz, C. Force, E. Comini, M. Manzanares, T. Andreu, A. Genç, J. Arbiol, P. Siciliano, G. Faglia, J.R. Morante, Surface modification of TiO<sub>2</sub> nanocrystals by WO<sub>x</sub> coating or wrapping: Solvothermal synthesis and enhanced surface chemistry, *ACS Appl. Mater. Interfaces* 7 (2015) 6898-6908.

- [37] W. Alammari, M. Govindhan, A. Chen, Modification of TiO<sub>2</sub> nanotubes with PtRu/graphene nanocomposites for enhanced oxygen reduction reaction, *ChemElectroChem* 2 (2015) 2041-2047.
- [38] H. Choi, D. Shin, B.C. Yeo, T. Song, S.S. Han, N. Park, S. Kim, Simultaneously controllable doping sites and the activity of a W–N codoped TiO<sub>2</sub> photocatalyst, *ACS Catal.* 6 (2016) 2745-2753.
- [39] M. Nolan, A. Iwaszuk, A.K. Lucid, J.J. Carey, M. Fronzi, Design of novel visible light active photocatalyst materials: Surface modified TiO<sub>2</sub>, *Adv. Mater.* DOI: 10.1002/adma.201504894 (2016) n/a-n/a.
- [40] J. Ni, S. Fu, C. Wu, J. Maier, Y. Yu, L. Li, Self-supported nanotube arrays of sulfur-doped TiO<sub>2</sub> enabling ultrastable and robust sodium storage, *Adv. Mater.* 28 (2016) 2259-2265.
- [41] S. Liu, J. Yu, Effect of F-Doping on the Photocatalytic Activity and Microstructures of Nanocrystalline TiO<sub>2</sub> Powders, in: H. Yamashita, H. Li (Eds.) *Nanostructured Photocatalysts: Advanced Functional Materials*, Springer International Publishing, Cham, 2016, pp. 187-200.
- [42] F. Marco, I. Anna, L. Aoife, N. Michael, Metal oxide nanocluster-modified TiO<sub>2</sub> as solar activated photocatalyst materials, *J. Phys.: Condens. Matter* 28 (2016) 074006.
- [43] S.A. Bakar, G. Byzinski, C. Ribeiro, Synergistic effect on the photocatalytic activity of N-doped TiO<sub>2</sub> nanorods synthesised by novel route with exposed (110) facet, *J. Alloys Compd.* 666 (2016) 38-49.
- [44] M.R. Bayati, A.Z. Moshfegh, F. Golestani-Fard, Micro-arc oxidized S-TiO<sub>2</sub> nanoporous layers: Cationic or anionic doping?, *Mater. Lett.* 64 (2010) 2215-2218.

- [45] V. Etacheri, M.K. Seery, S.J. Hinder, S.C. Pillai, Oxygen rich titania: A dopant free, high temperature stable, and visible-light active anatase photocatalyst, *Adv. Funct. Mater.* 21 (2011) 3744-3752.
- [46] D. Pei, J. Luan, Development of visible light-responsive sensitized photocatalysts, *Int. J. Photoenergy* 2012 (2012) 13.
- [47] L.-L. Tan, W.-J. Ong, S.-P. Chai, A.R. Mohamed, Band gap engineered, oxygen-rich TiO<sub>2</sub> for visible light induced photocatalytic reduction of CO<sub>2</sub>, *Chem. Commun.* 50 (2014) 6923-6926.
- [48] L.-L. Tan, W.-J. Ong, S.-P. Chai, A.R. Mohamed, Visible-light-activated oxygen-rich TiO<sub>2</sub> as next generation photocatalyst: Importance of annealing temperature on the photoactivity toward reduction of carbon dioxide, *Chem. Eng. J.* 283 (2016) 1254-1263.
- [49] W.-J. Ong, L.-L. Tan, S.-P. Chai, S.-T. Yong, A.R. Mohamed, Self-assembly of nitrogen-doped TiO<sub>2</sub> with exposed {001} facets on a graphene scaffold as photo-active hybrid nanostructures for reduction of carbon dioxide to methane, *Nano Res.* 7 (2014) 1528-1547.
- [50] L.-L. Tan, S.-P. Chai, A.R. Mohamed, Synthesis and applications of graphene-based TiO<sub>2</sub> photocatalysts, *ChemSusChem* 5 (2012) 1868-1882.
- [51] Y. Ji, Y. Luo, Theoretical study on the mechanism of photoreduction of CO<sub>2</sub> to CH<sub>4</sub> on the anatase TiO<sub>2</sub>(101) surface, *ACS Catal.* 6 (2016) 2018-2025.
- [52] Y. Kohno, T. Tanaka, T. Funabiki, S. Yoshida, Reaction mechanism in the photoreduction of CO<sub>2</sub> with CH<sub>4</sub> over ZrO<sub>2</sub>, *Phys. Chem. Chem. Phys.* 2 (2000) 5302-5307.

- [53] M. Tahir, N.S. Amin, Photocatalytic reduction of carbon dioxide with water vapors over montmorillonite modified TiO<sub>2</sub> nanocomposites, *Appl. Catal., B* 142–143 (2013) 512-522.
- [54] M. Tahir, N.S. Amin, Photocatalytic CO<sub>2</sub> reduction and kinetic study over In/TiO<sub>2</sub> nanoparticles supported microchannel monolith photoreactor, *Appl. Catal., A* 467 (2013) 483-496.
- [55] K. Kočí, L. Obalová, L. Matějová, D. Plachá, Z. Lacný, J. Jirkovský, O. Šolcová, Effect of TiO<sub>2</sub> particle size on the photocatalytic reduction of CO<sub>2</sub>, *Appl. Catal., B* 89 (2009) 494-502.
- [56] J.-C. Wang, L. Zhang, W.-X. Fang, J. Ren, Y.-Y. Li, H.-C. Yao, J.-S. Wang, Z.-J. Li, Enhanced photoreduction CO<sub>2</sub> activity over direct Z-Scheme -Fe<sub>2</sub>O<sub>3</sub>/Cu<sub>2</sub>O heterostructures under visible light irradiation, *ACS Appl. Mater. Interfaces* 7 (2015) 8631-8639.
- [57] I. Tseng, W.C. Chang, J. Wu, Photoreduction of CO<sub>2</sub> using sol–gel derived titania and titania-supported copper catalysts, *Appl. Catal., B* 37 (2002) 37-48.
- [58] Y. Li, W.-N. Wang, Z. Zhan, M.-H. Woo, C.-Y. Wu, P. Biswas, Photocatalytic reduction of CO<sub>2</sub> with H<sub>2</sub>O on mesoporous silica supported Cu/TiO<sub>2</sub> catalysts, *Appl. Catal., B* 100 (2010) 386-392.
- [59] Z. Zhao, J. Fan, J. Wang, R. Li, Effect of heating temperature on photocatalytic reduction of CO<sub>2</sub> by N–TiO<sub>2</sub> nanotube catalyst, *Catalysis Communications* 21 (2012) 32-37.
- [60] K. Kočí, K. Zatloukalová, L. Obalová, S. Krejčíková, Z. Lacný, L. Špek, A. Hospodková, O. Šolcová, Wavelength effect on photocatalytic reduction of CO<sub>2</sub> by Ag/TiO<sub>2</sub> catalyst, *Chin. J. Catal.* 32 (2011) 812-815.

- [61] J.C.S. Wu, H.-M. Lin, C.-L. Lai, Photo reduction of CO<sub>2</sub> to methanol using optical-fiber photoreactor, *Appl. Catal., A* 296 (2005) 194-200.
- [62] C.-C. Lo, C.-H. Hung, C.-S. Yuan, J.-F. Wu, Photoreduction of carbon dioxide with H<sub>2</sub> and H<sub>2</sub>O over TiO<sub>2</sub> and ZrO<sub>2</sub> in a circulated photocatalytic reactor, *Sol. Energy Mater. Sol. Cells* 91 (2007) 1765-1774.
- [63] T. Kentaro, T. Tsunehiro, Photocatalytic reduction of CO<sub>2</sub> using H<sub>2</sub> as reductant over solid base photocatalysts, *Advances in CO<sub>2</sub> Conversion and Utilization*, American Chemical Society 2010, pp. 15-24.
- [64] K. Teramura, T. Tanaka, H. Ishikawa, Y. Kohno, T. Funabiki, Photocatalytic reduction of CO<sub>2</sub> to CO in the presence of H<sub>2</sub> or CH<sub>4</sub> as a reductant over MgO, *J. Phys. Chem. B* 108 (2003) 346-354.
- [65] M. Tahir, N.S. Amin, Indium-doped TiO<sub>2</sub> nanoparticles for photocatalytic CO<sub>2</sub> reduction with H<sub>2</sub>O vapors to CH<sub>4</sub>, *Appl. Catal., B* 162 (2015) 98-109.
- [66] W.S. Hummers, R.E. Offeman, Preparation of graphitic oxide, *J. Am. Chem. Soc.* 80 (1958) 1339-1339.
- [67] Y. Ku, W.-H. Lee, W.-Y. Wang, Photocatalytic reduction of carbonate in aqueous solution by UV/TiO<sub>2</sub> process, *J. Mol. Catal. A: Chem.* 212 (2004) 191-196.
- [68] B.K. Sharma, R. Ameta, J. Kaur, S.C. Ameta, Photocatalytic reduction of carbon dioxide over ferrocyanide-coated titanium dioxide powder, *International Journal of Energy Research* 21 (1997) 923-929.
- [69] W. Lin, H. Han, H. Frei, CO<sub>2</sub> splitting by H<sub>2</sub>O to CO and O<sub>2</sub> under UV light in TiMCM-41 silicate sieve, *J. Phys. Chem. B* 108 (2004) 18269-18273.



- [70] W.-H. Lee, C.-H. Liao, M.-F. Tsai, C.-W. Huang, J.C.S. Wu, A novel twin reactor for CO<sub>2</sub> photoreduction to mimic artificial photosynthesis, *Appl. Catal., B* 132–133 (2013) 445–451.
- [71] S. Kaneco, H. Kurimoto, Y. Shimizu, K. Ohta, T. Mizuno, Photocatalytic reduction of CO<sub>2</sub> using TiO<sub>2</sub> powders in supercritical fluid CO<sub>2</sub>, *Energy* 24 (1999) 21–30.
- [72] M. Anpo, H. Yamashita, Y. Ichihashi, Y. Fujii, M. Honda, Photocatalytic reduction of CO<sub>2</sub> with H<sub>2</sub>O on titanium oxides anchored within micropores of zeolites: effects of the structure of the active sites and the addition of Pt, *J. Phys. Chem. B* 101 (1997) 2632–2636.
- [73] B. Tahir, M. Tahir, N.S. Amin, Performance analysis of monolith photoreactor for CO<sub>2</sub> reduction with H<sub>2</sub>, *Energy Convers. Manage.* 90 (2015) 272–281.
- [74] M.O. Reese, S.A. Gevorgyan, M. Jørgensen, E. Bundgaard, S.R. Kurtz, D.S. Ginley, D.C. Olson, M.T. Lloyd, P. Morvillo, E.A. Katz, A. Elschner, O. Haillant, T.R. Currier, V. Shrotriya, M. Hermenau, M. Riede, K. R. Kirov, G. Trimmel, T. Rath, O. Inganäs, F. Zhang, M. Andersson, K. Tvingstedt, M. Lira-Cantu, D. Laird, C. McGuinness, S. Gowrisanker, M. Pannone, M. Xiao, J. Hauch, R. Steim, D.M. DeLongchamp, R. Rösch, H. Hoppe, N. Espinosa, A. Urbina, G. Yaman-Uzunoglu, J.-B. Bonekamp, A.J.J.M. van Breemen, C. Girotto, E. Voroshazi, F.C. Krebs, Consensus stability testing protocols for organic photovoltaic materials and devices, *Sol. Energy Mater. Sol. Cells* 95 (2011) 1253–1267.
- [75] J.L. Sommerdijk, A. Bril, A.W. de Jager, Two photon luminescence with ultraviolet excitation of trivalent praseodymium, *J. Lumin.* 8 (1974) 341–343.
- [76] P. Harriott, *Chemical reactor design*, Marcel Dekker Inc, New York, NY, 2003.

- [77] G. Wang, B. Wang, J. Park, J. Yang, X. Shen, J. Yao, Synthesis of enhanced hydrophilic and hydrophobic graphene oxide nanosheets by a solvothermal method, *Carbon* 47 (2009) 68-72.
- [78] J. Wu, H. Li, X. Qi, Q. He, B. Xu, H. Zhang, Graphene oxide architectures prepared by molecular combing on hydrophilic-hydrophobic micropatterns, *Small* 10 (2014) 2239-2244.
- [79] L. Sirghi, Y. Hatanaka, Hydrophilicity of amorphous TiO<sub>2</sub> ultra-thin films, *Surface Science* 530 (2003) L323-L327.
- [80] S.S. Tan, L. Zou, E. Hu, Photocatalytic reduction of carbon dioxide into gaseous hydrocarbon using TiO<sub>2</sub> pellets, *Catal. Today* 115 (2006) 269-273.

ACCEPTED MANUSCRIPT

**Highlights**

- CO<sub>2</sub> photoreduction was conducted over graphene oxide/ oxygen-rich TiO<sub>2</sub> under visible light.
- Process parameters such as light intensity as well as CO<sub>2</sub> and H<sub>2</sub>O partial pressures were studied.
- A methane yield of 3.45 μmol g<sub>cat</sub><sup>-1</sup> was obtained at the most suitable process conditions.
- Kinetic studies of CO<sub>2</sub> photoreduction over graphene oxide/ oxygen-rich TiO<sub>2</sub> were presented.
- The experimental data was successfully fitted into a dual-site Langmuir-Hinshelwood model.

ACCEPTED MANUSCRIPT

## Graphical Abstract

